product yields, etc.). The same is equally true of the work described in this paper. Although TRIR has played a key role in unravelling the mechanism of these reactions, the results of many other experiments including the flash photolysis[4] of $[CpFe(CO)_2]_2$, the characterization of $Cp_2Fe_2(CO)_3$ in low-temperature matrices,[5,6] and measurements of quantum yields[21,22b] have been important in constructing the complete mechanism shown in the schemes. The great strength of TRIR, however, is that the narrow line width of $\nu$(C-O) bands allows one to monitor each intermediate in real time in the reaction mixture, thus reducing the need to speculate when devising the overall mechanism for a reaction. TRIR has now been applied to the reactions of a number of related dinuclear complexes,[53] and we are currently extending this work to establish whether the behavior of $[CpFe(CO)_2]_2$ is typical of such compounds.

**Acknowledgment.** We thank SERC, the EC Science Program (Contract ST0007), NATO (Grant No. 900544), the Petroleum Research Fund, administered by the American Chemical Society, the Paul Instrument Fund of the Royal Society, Mütek GmbH, Perkin-Elmer Ltd., and BP International Ltd for their financial support. We are grateful to Dr. S. Firth, Dr. S. A. Gravelle, Dr. M. A. Healy, Dr. P. M. Hodges, Dr. S. M. Howdle, Ms. M. Jobling, Mr. F. P. Johnson, Dr. B. D. Moore, Professor R. N. Perutz, Professor N. Sheppard, Dr. L. J. Van der Burgt, and Dr. A. H. Wright for their help and advice. We thank Professor E. Weitz, Professor J. M. Kelly, and Dr. C. Long for access to equipment in their laboratories. Finally, we thank Mr. D. R. Dye, Mr. J. G. Gamble, Mr. D. Lichfield, Mr. R. Parsons, Mr. W. E. Porter, and Mr. J. M. Whalley for their continued assistance in developing and building the TRIR equipment at Nottingham.

**Registry No. 3**, 87985-70-4; $[CpFe(CO)_2]_2$, 12154-95-9; $CpFe(CO)_2$, 55009-40-0; $Cp_2Fe(CO)_3(THF)$, 138489-71-1; $CpFe(CO)P(OMe)_3$, 113843-93-9; $CpFe(CO)PO^iPr)_3$, 138489-74-4; $CpFe(CO)P(OEt)_3$, 138489-75-5; $Cp_2Fe_2(CO)_3P(OMe)_3$, 33087-08-0; $Cp_2Fe_2(CO)_3P(OEt)_3$, 33057-34-0; $Cp_2Fe_2(CO)_3P(O^iPr)_3$, 33218-96-1; $[CpFe(CO)P(OMe)_3]_2$, 71579-40-3; $[CpFe(CO)P(O^iPr)_3]_2$, 138489-72-2; $[CpFe(CO)P(OEt)_3]_2$, 138489-73-3.

# Polymorphism of 1,3-Phenylene Bis(diselenadiazolyl). Solid-State Structural and Electronic Properties of $\beta$-1,3-$[(Se_2N_2C)C_6H_4(CN_2Se_2)]$

**A. W. Cordes,*[1a] R. C. Haddon,*[1b] R. G. Hicks,[1c] R. T. Oakley,*[1c] T. T. M. Palstra,[1b] L. F. Schneemeyer,[1b] and J. V. Waszczak[1b]**

*Contribution from the Department of Chemistry and Biochemistry, University of Arkansas, Fayetteville, Arkansas 72701, AT&T Bell Laboratories, Murray Hill, New Jersey 07974, and Guelph Waterloo Centre for Graduate Work in Chemistry, Guelph Campus, Department of Chemistry and Biochemistry, University of Guelph, Guelph, Ontario N1G 2W1, Canada.*
*Received August 12, 1991*

**Abstract:** The solid-state characterization of a second or $\beta$-phase of the 1,3-phenylene-bridged diselenadiazolyl diradical 1,3-$[(Se_2N_2C)C_6H_4(CN_2Se_2)]$ is reported. Crystals of this $\beta$-phase are monoclinic, space group $P2_1/n$, with $a$ = 9.108 (6), $b$ = 15.233 (13), $c$ = 16.110 (5) Å, $\beta$ = 103.37 (5)°, $Z$ = 8. The crystal structure consists of chain-like arrays of discrete dimers (4 per unit cell), although one intradimer Se-Se linkage is notably longer (3.411 Å) than the other three (3.125, 3.196, 3.204 Å). The dimer units lie in chains that are linked by a complex three-dimensional array of Se-Se contacts. Variable-temperature single-crystal conductivity measurements on this phase indicate a band gap of 0.77 eV. Consistent with the conductivity measurements, extended Hückel band structure calculations suggest a relatively isotropic electronic structure.

## Introduction

Our interest[2] in the construction of molecular conductors from neutral $\pi$-radicals has prompted us to investigate the use of thiazyl and selenazyl radicals as molecular building blocks. Of the various radical derivatives that have been explored,[3,4] those based on the 1,2,3,5-dithia- and 1,2,3,5-diselenadiazolyl ring systems are particularly appealing as precursors for new materials.[5,6] Toward this end we recently described the preparation and solid-state structural and electronic properties of the 1,3- and 1,4-phenylene-bridged bis(dithiadiazolyl) and bis(diselenadiazolyl) diradicals $[(E_2N_2C)C_6H_6(CN_2E_2)]$ **1**[7] and **2**[8] (E = S, Se). In the

(1) (a) University of Arkansas. (b) AT&T Bell Laboratories. (c) University of Guelph.

(2) (a) Haddon, R. C. *Nature (London)* **1975**, *256*, 394. (b) Haddon, R. C. *Aust. J. Chem.* **1975**, *28*, 2343.

(3) (a) Wolmershäuser, G.; Schnauber, M.; Wilhelm, T. *J. Chem. Soc., Chem. Commun.* **1984**, 573. (b) Wolmershäuser, G.; Schnauber, M.; Wilhelm, T.; Sutcliffe, L. H. *Synth. Met.* **1986**, *14*, 239. (c) Dormann, E.; Nowak, M. J.; Williams, K. A.; Angus, R. O., Jr.; Wudl, F. *J. Am. Chem. Soc.* **1987**, *109*, 2594. (d) Wolmershäuser, G.; Wortmann, G.; Schnauber, M. *J. Chem. Res. Synop.* **1988**, 358. (e) Wolmershäuser, G.; Johann, R. *Angew. Chem., Int. Ed. Engl.* **1989**, *28*, 920. (f) Hayes, P. J.; Oakley, R. T.; Cordes, A. W.; Pennington, W. T. *J. Am. Chem. Soc.* **1985**, *107*, 1346. (g) Boerē, R. T.; Cordes, A. W.; Hayes, P. J.; Oakley, R. T.; Reed, R. W. *Inorg. Chem.* **1986**, *25*, 2445. (h) Oakley, R. T.; Reed, R. W.; Cordes, A. W.; Craig, S. L.; Graham, J. B. **1987**, *109*, 7745. (i) Boerē, R. T.; French, C. L.; Oakley, R. T.; Cordes, A. W.; Privett, J. A. J.; Craig, S. L.; Graham, J. B. *J. Am. Chem. Soc.* **1985**, *107*, 7710. (j) Awere, E. G.; Burford, N.; Haddon, R. C.; Parsons, S.; Passmore, J.; Waszczak, J. V.; White, P. S. *Inorg. Chem.* **1990**, *29*, 4821. (k) Banister, A. J.; Rawson, J. M.; Clegg, W.; Birkby, S. L. *J. Chem. Soc., Dalton Trans.* **1991**, 1099.

(4) Cordes, A. W.; Haddon, R. C.; Oakley, R. T. In *The Chemistry of Inorganic Ring Systems*; Steudel, R., Ed.; Elsevier: Amsterdam, 1992.

(5) Vegas, A.; Perēz-Salazar, A.; Banister, A. J.; Hey, R. G. *J. Chem. Soc., Dalton Trans.* **1980**, 1812. (b) Hofs, H.-U.; Bats, J. W.; Gleiter, R.; Hartmann, G.; Mews, R.; Eckert-Maksič, M.; Oberhammer, H.; Sheldrick, G. M. *Chem. Ber.* **1985**, *118*, 3781. (c) Fairhurst, S. A.; Johnson, K. M.; Sutcliffe, L. H.; Preston, K. F.; Banister, A. J.; Hauptmann, Z. V.; Passmore, J. *J. Chem. Soc., Dalton Trans.* **1986**, 1465. (d) Boerē, R. T.; Oakley, R. T.; Reed, R. W.; Westwood, N. P. C. *J. Am. Chem. Soc.* **1989**, *111*, 1180. (e) Banister, A. J.; Hansford, M. I.; Hauptmann, Z. V.; Wait, S. T.; Clegg, W. *J. Chem. Soc., Dalton Trans.* **1989**, 1705. (f) Cordes, A. W.; Goddard, J. D.; Oakley, R. T.; Westwood, N. P. C. *J. Am. Chem. Soc.* **1989**, *111*, 6147.

(6) Del Bel Belluz, P.; Cordes, A. W.; Kristof, E. M.; Kristof, P. V.; Liblong, S. W.; Oakley, R. T. *J. Am. Chem. Soc.* **1989**, *111*, 9276.

(7) Andrews, M. P.; Cordes, A. W.; Douglass, D. C.; Fleming, R. M.; Glarum, S. H.; Haddon, R. C.; Marsh, P.; Oakley, R. T.; Palstra, T. T. M.; Schneemeyer, L. F.; Trucks, G. W.; Tycko, R.; Waszczak, J. V.; Young, K. M.; Zimmerman, N. M. *J. Am. Chem. Soc.* **1991**, *113*, 3559.

0002-7863/92/1514-1729$03.00/0 

**Table I.** Unit Cell Parameters for $\alpha$- and $\beta$-Phases of **1** (E = Se) and Selected Structural Data (Distances in Å)

| phase | space group | $a$ | $b$ | $c$ | $\beta$ (deg) |
|---|---|---|---|---|---|
| $\alpha$ | $I4_1/a$ | 34.617 (13) | | 7.228 (4) | |
| $\beta$ | $P2_1/n$ | 9.108 (6) | 15.233 (13) | 16.110 (5) | 103.37 (5) |

Selected Distances in $\beta$-Phase

| | | | |
|---|---|---|---|
| Se1–Se2 | 2.345 (3) | Se3–Se4 | 2.321 (3) |
| Se5–Se6 | 2.344 (3) | Se7–Se8 | 2.335 (3) |
| Se1–Se7 | 3.204 (3) | Se2–Se8 | 3.196 (3) |
| Se3–Se5 | 3.125 (3) | Se4–Se6 | 3.411 (3) |
| $d_1$ (Se2–Se8′) | 3.859 (3) | $d_4$ (Se6–Se7′) | 3.865 (3) |
| $d_2$ (Se3–Se3′) | 3.979 (3) | $d_5$ (Se7–Se8′) | 3.816 (3) |
| $d_3$ (Se6–Se8′) | 3.779 (3) | | |

solid state the former stack in a vertical fashion with individual "plates" linked by a zigzag network of E–E contacts, i.e., **3**. The latter stack as interleaved arrays of diradical dimers, i.e., **4**.

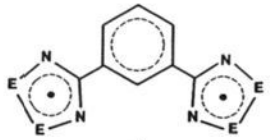


**1**


**2**

**3**

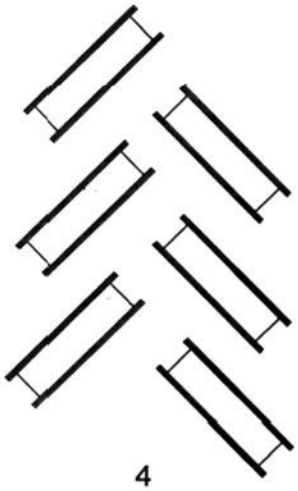

**4**

During our work on the physical characterization of these species we have discovered that the 1,3-selenium derivative **1** (E = Se) can also be generated in a second or $\beta$-phase. Herein we report the structural characterization of this new phase and compare its magnetic and conductivity properties with those of the previously described $\alpha$-phase **3**. The results are discussed in the light of extended Hückel band structure calculations.

## Results and Discussion

**Crystal Structure.** Golden blocks of $\beta$-1,3-[$(Se_2N_2C)C_6H_4(CN_2Se_2)$] *are monoclinic, space group* $P2_1/n$. *Unit cell parameters* for this second phase (as well as those of the $\alpha$-phase) are summarized in Table I, along with selected internuclear distance information. In the $\beta$-phase the diradicals associate into dimeric units, with four dimers to the unit cell. An ORTEP drawing of a single dimer unit is shown in Figure 1. The internal structural parameters of the dimers are similar to those seen in other diselenadiazolyl structures.[6-8] There is, however, one unusual feature regarding the intradimer Se–Se contacts; while Se1–Se7, Se2–Se8, and Se3–Se5 are similar to those seen before, the Se4–Se6 linkage is significantly longer.

There is no indication of the kind of molecular stacking found in either the $\alpha$-phase or the 1,4-derivative **4**. Instead the crescent-shaped dimers coil together to produce chain-like arrays

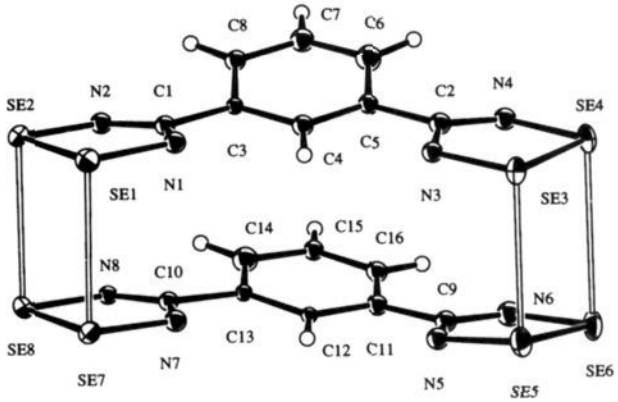


**Figure 1.** A single dimer unit in the $\beta$-phase of **1** (E = Se), with atom numbering.

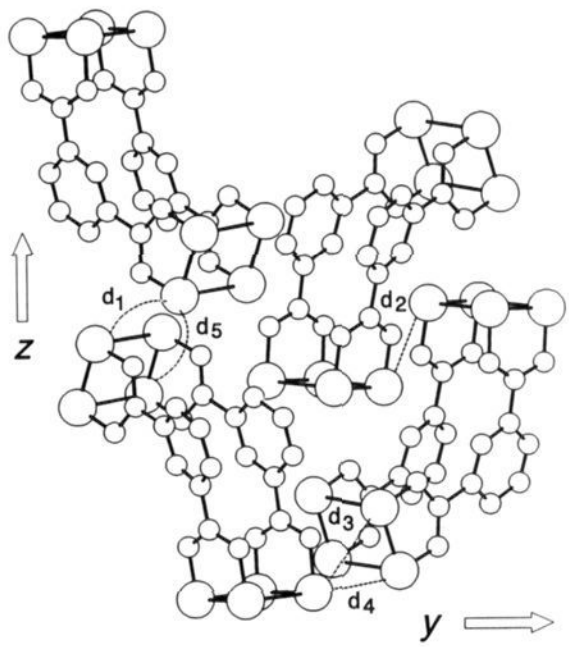


**Figure 2.** A schematic view of the chain-like arrangement of dimers in the $yz$ plane. Shaded molecules lie slightly below and unshaded molecules slightly above the plane of the paper. Short interdimer Se–Se contacts (as defined in Figure 4 and Table I) are shown as dashed lines.

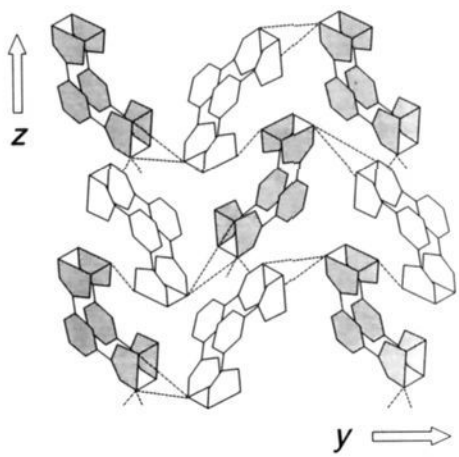


**Figure 3.** A local view of the packing in the $yz$ plane and definition of the contacts $d_1$–$d_5$.

parallel to the $z$ axis (see Figure 2). The molecular packing gives rise to a complex three-dimensional network of close interdimer Se–Se contacts. Within the chains every diradical dimer has two

(8) Cordes, A. W.; Haddon, R. C.; Oakley, R. T.; Schneemeyer, L. F.; Waszczak, J. V.; Young, K. M.; Zimmerman, N. M. *J. Am. Chem. Soc.* **1991**, *113*, 582.

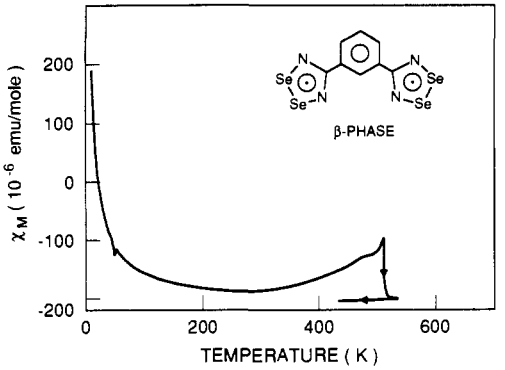


**Figure 4.** Magnetic susceptibility of the β-phase of **1** (E = Se) as a function of temperature.

**Table II.** Magnetic and Conductivity Parameters for the α- and β-Phases of **1** (E = Se)

| phase | α[a] | β |
|---|---|---|
| concn of defects (% per molecule) | 0.51 | 1.31 |
| θ (K) | −1 | 1 |
| diamagnetism (ppm emu $mol^{-1}$) | −164 | −219 |
| band gap (eV) | 0.55 | 0.77 |
| carrier density (per molecule, at 300 K) | $1.3 \times 10^{-6}$ | $1.8 \times 10^{-8}$ |
| mobility ($cm^2 V^{-1} s^{-1}$, at 300 K) | 2.2 | 150 |

[a] From ref 7.

nearest neighbors, one based on a convex and the other a concave approach of two dimers; each of these arrangements straddles a crystallographic inversion center. The close Se–Se contacts $d_1$, $d_2$, and $d_5$ arising from these approaches, illustrated schematically in Figure 3 and crystallographically in Figure 3, provide the "links" along the chains. It should be noted that $d_1$ and $d_5$ are not to the same dimer unit; the former is between Se8′ and Se2 in a radical unit above it, while the latter is from Se8′ to Se7 in a radical beneath it. The third type of interdimer contact, characterized by the distances $d_3$ and $d_4$, represents the approach of one dimer to the underside of another. Both of these contacts, which are reminiscent of the butt-end contacts observed in the 1,4-structures **4**, involve the same atom (Se6) with the longest intradimer bond (3.411 Å). These final contacts provide a mechanism for orbital interactions between adjacent molecular chains.

**Magnetic Susceptibility and Conductivity Measurements.** The measured magnetic susceptibility of the β-phase of **1** (E = Se) as a function of temperature is shown in Figure 4. The low-temperature susceptibility shows Curie behavior, due to a small concentration of defects, which are associated with unpaired electrons. The concentration of paramagnetic defects, along with the θ value and measured diamagnetism for both the α- and β-phases, are given in Table II. Log plots of the single-crystal conductivity of the two phases are shown in Figure 5. If, as before,[7] we treat the material as an intrinsic semiconductor, we obtain the conductivity parameters listed in Table II. In contrast to the needle-like appearance of the α-phase, the morphology of the β-phase allowed us to use the van der Pauw technique for conductivity measurements; these indicated that the conductivity of the latter phase is isotropic in the two dimensions examined. The conductivity behavior of the two phases is rather similar. The higher mobility of the β-phase may be a reflection of the isotropic nature of this phase.

**Band Structure Calculations.** Three-dimensional band structure calculations were performed using extended Hückel methods with a parameterization scheme described previously.[8] As illustrated by the density of states curves shown in Figure 6, and in accord with the conductivity measurements, there is a substantial band gap at the Fermi level for β-phase. The calculated band gap of 1.2 eV is larger than that predicted for the α-phase (0.8 eV). The β-phase is, however, more isotropic than the α-phase.

**Summary and Conclusions.** In our search for neutral molecular materials which possess the desirable structural, thermal and electronic properties for electronic conduction we have explored

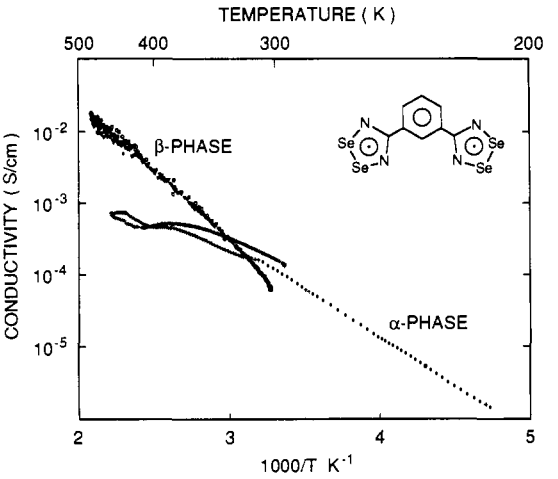


**Figure 5.** Log plot of single-crystal conductivities of α- and β-phases of **1** (E = Se) as a function of inverse temperature.

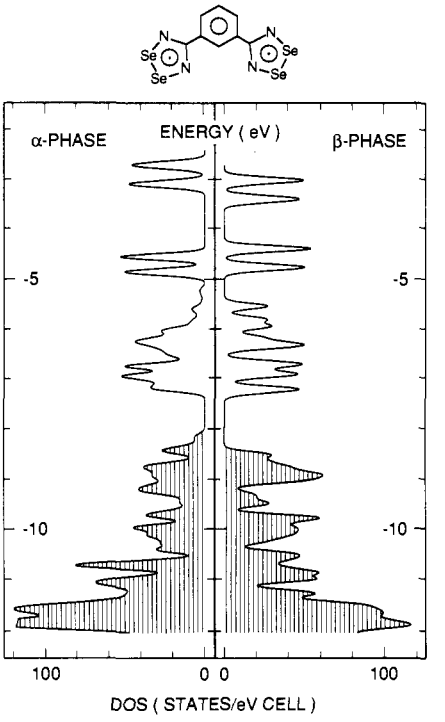


**Figure 6.** Calculated density of states for the β-phase of **1** (E = Se).

the properties of 1,3- and 1,4-phenylene-bridged bis(dithiadiazolyl) and bis(diselenadiazolyl) diradicals. We have previously shown that, in the case of the α-phase of the 1,3-diradical system **1**, the desired 1-dimensional stacking of molecular units, i.e., **3**, can be induced. The results provided herein suggest that this latter morphology carries no particular energetic advantage, indeed the stacked α-phase is metastable at elevated temperatures with respect to the chain-like β-phase. This latter phase shows a weaker but more three-dimensional network of Se–Se contacts than the α-phase. Both phases show conductivity/temperature characteristics of intrinsic materials. As expected, the conductivity of the β-phase is lower and the band gap higher than that of the α-phase.

## Experimental Section

**Crystal Growth.** Preparative details for **1** (E = Se) have been described in an earlier paper.[7] During our initial studies small, golden needle-like crystals of the α-phase (i.e., **3**) were grown by slow sublimation (over several weeks) at $10^{-6}$ Torr. The material to be sublimed was heated in a glass vessel seated in an aluminum block heated to 180 °C; crystals were deposited on a glass finger maintained near 100 °C. More recently we have found that, if higher pressures are used, e.g., $10^{-1}$–$10^{-2}$ Torr, a block temperature near 220 °C must be used to effect vaporization. By using a finger temperature near 120–140 °C, a mixture

of needles of the $\alpha$-phase and blocks of the new $\beta$-phase is produced; the two phases can be separated manually. The $\alpha$-phase is more volatile; it can be resublimed under less extreme conditions and tends to vaporize from a heated finger more readily than the $\beta$-phase: dec ($\beta$-phase) >350 °C; infrared spectrum ($\beta$-phase, 1600–250 $cm^{-1}$ region) 1331 (m), 1307 (s), 1281 (m), 1255 (w), 1247 (w), 1142 (m), 1079 (w), 1068 (w), 919 (w), 805 (w), 796 (w), 750 (m), 733 (m), 688 (vs), 678 (vs), 649 (m), 616 (s), 391 (s) $cm^{-1}$.

**X-ray Measurements.** A brass-colored block of the $\beta$-phase of **1** was mounted on a glass fiber and coated with epoxy. X-ray data were collected on an ENRAF-Nonius CAD-4 at 293 K with monochromated Mo $K_\alpha$ ($\lambda$ = 0.71073 Å radiation) to a $2\theta_{max}$ of 23°. A $\psi$-scan absorption correction varied from 0.58–1.00. The structure was solved using MULTAN and refined by full-matrix least squares which minimized $\sum w(\Delta F)^2$. In the final full-matrix least-squares refinement $R$ = 0.042 for 1346 reflections ($I > 3\sigma(I)$) and 169 parameters (C and N atoms were refined isotropically). H atoms were constrained to idealized positions (C–H = 0.95 Å) with isotropic $B$ values of 1.2 times $B_{eq}$ of the attached C atom. Data collection, structure solution, and refinement parameters are available as supplementary material.

**Conductivity Measurements.** The conductivity measurements were performed with a Keithley 236 unit. Whereas the needle-like $\alpha$-phase allowed a reliable four-point-probe bar geometry, the platelet samples of the $\beta$-phase were measured with the van der Pauw technique. The resulting error in comparisons between the two phases could be up to a factor of 2 as a result of the geometrical factor. The four contacts were made with gold paint, resulting in a contact resistance that was at least two orders of magnitude higher than the sample resistance. This limited the temperature window of the measurements. The contact resistance decreased on heating the sample, which might be the origin of the scatter in the data points in Figure 6. The carrier density and mobility were calculated by assuming that the carriers were due to thermal activation across the band (intrinsic semiconductor).[7] It should be noted that small errors in the determination of the energy gap propagate exponentially in the derivation of the mobility and carrier density.

**Magnetic Susceptibility Measurements.** The magnetic susceptibility was measured from 4.2 to 550 K using the Faraday technique. Details of this apparatus have been previously described.[9] The applied field was 14 kOe, and the measured susceptibility was checked for field dependence at several temperatures.

**Band Structure Calculations.** The band structures were carried out with the EHMACC suite of programs using parameters discussed previously.[8a,10] The off-diagonal elements of the Hamiltonian matrix were calculated with the standard weighting formula.[11]

**Acknowledgment.** Financial support at Guelph was provided by the Natural Sciences and Engineering Research Council of Canada and at Arkansas by the National Science Foundation (EPSCOR program) and the State of Arkansas.

**Supplementary Material Available:** Tables of crystal data, structure solution, and refinement (S1), atomic coordinates (S2), bond lengths and angles (S3), and anisotropic thermal parameters (S3) for $\beta$-1,3-[$(Se_2N_2C)C_6H_4(CN_2Se_2)$] (7 pages). Ordering information is given on any current masthead page.

(9) (a) DiSalvo, F. J.; Waszczak, J. V. *Phys. Rev.* **1981**, *B23*, 457. (b) DiSalvo, F. J.; Menth, A.; Waszczak, J. V.; Tauc, J. *Phys. Rev.* **1972**, *B6*, 4574.

(10) Basch, H.; Viste, A.; Gray, H. B. *Theor. Chim. Acta* **1965**, *3*, 458.

(11) Ammeter, J. H.; Burghi, H. B.; Thibeault, J. C.; Hoffmann, R. *J. Am. Chem. Soc.* **1978**, *100*, 3686.

# Redistribution of Reduced Thiophene Ligands in the Conversion of $(C_5R_5)Rh(\eta^4\text{-}C_4Me_4S)$ to $[(C_5R_5)Rh]_3(\eta^4,\eta^1\text{-}C_4Me_4S)_2$

**Shifang Luo, Anton E. Skaugset, Thomas B. Rauchfuss,* and Scott R. Wilson**

*Contribution from the School of Chemical Sciences, University of Illinois, Urbana, Illinois 61801.*
*Received July 8, 1991*

**Abstract:** The thermal decomposition of $(C_5Me_5)Rh(\eta^4\text{-}C_4Me_4S)$ (**1**) has been examined by spectroscopic, kinetic, and structural studies. Compound **1** cleanly eliminates free $C_4Me_4S$ to give $[(C_5Me_5)Rh]_3(\eta^4,\eta^1\text{-}C_4Me_4S)_2$ (**2a**). The structure of the analogous compound $[(C_5Me_4Et)Rh]_3(\eta^4,\eta^1\text{-}C_4Me_4S)_2$ (**2b**) consists of a pair of $(C_5Me_4Et)Rh(\eta^4\text{-}C_4Me_4S)$ ligands bound to a central $(C_5Me_4Et)Rh^I$ unit through the sulfur atoms. The conversion of **1** to **2a** occurs via a second-order process (in rhodium) with $k$(60 °C) = 3.94 × $10^{-4}$ $M^{-1}\cdot s^{-1}$ which implicates an associative mechanism. Activation parameters are $\Delta H^\ddagger$ = 20.1 ± 0.1 kcal/mol and $\Delta S^\ddagger$ = −13.9 ± 3.1 cal/mol·K. Dynamic $^1H$ NMR studies demonstrate that **2a** maintains its structure in solution but that it experiences restricted rotation about the two Rh–S bonds. Compound **2a** decomposes via a first-order process with $k$(100 °C) = 8.94 × $10^{-6}$ $s^{-1}$ to give $(C_5Me_5)_2Rh_2C_4Me_4S$, **3**.

## Introduction

The chemistry of thiophene–metal interactions has been of recent interest with emphasis on structural and reactivity principles.[1] A large number of thiophene complexes has been prepared in recent years, and several bonding modes have been identified.[2] Studies on thiophene complexation have been motivated by intense interest in the molecular mechanisms of the industrially important hydrodesulfurization process (HDS).[3] In HDS liquid fossil fuels are subjected to catalytic hydrogenation conditions with the goal of cleaving the constituent C–S bonds to give a sulfur-free hydrocarbon. Thiophene derivatives are particularly common constituents in fossil fuels[4] and are of special interest because of

(1) Rauchfuss, T. B. *Prog. Inorg. Chem.* **1991**, *39*, 259. Angelici, R. J. *Coord. Chem. Rev.* **1990**, *105*, 61. Angelici, R. J. *Acc. Chem. Res.* **1988**, *21*, 387.

(2) Some recent studies of thiophene complexes: (a) Ganja, E. A.; Rauchfuss, T. B.; Wilson, S. R. *Organometallics* **1991**, *10*, 270. (b) Jones, W. D.; Dong, L. *J. Am. Chem. Soc.* **1991**, *113*, 559. (c) Wang, D.-L.; Hwang, W.-S. *J. Organomet. Chem.* **1991**, *406*, C29. (d) Riaz, U.; Curnow, O.; Curtis, M. D. *J. Am. Chem. Soc.* **1991**, *113*, 1416. (e) Clark, P. D.; Fait, J. F.; Jones, C. G.; Kirk, M. J. *Can. J. Chem.* **1991**, *69*, 590. (f) Choi, M.-G.; Robertson, M. J.; Angelici, R. J. *J. Am. Chem. Soc.* **1991**, *113*, 4005.

(3) Gates, B. C.; Katzer, J. R.; Schuit, G. C. A. *Chemistry of Catalytic Processes*; McGraw-Hill: New York, 1979. Zonnevylle, M. C.; Hoffmann, R.; Harris, S. *Surf. Sci.* **1988**, *199*, 320. Harris, S.; Chianelli, R. R. *J. Catalysis* **1986**, *98*, 17.

(4) *Geochemistry of Sulfur in Fossil Fuels*; Orr, W. L., White, C. M., Eds.; American Chemical Society: Washington, DC, 1990. Galperin, G. D. *Chemistry of Heterocyclic Compounds*; Gronowitz, S., Ed.; John Wiley & Sons, Inc.: New York, 1986; Vol. 44, Part 1, p 325.

0002-7863/92/1514-1732$03.00/0 